Fatigue Crack Paths in AA2024-T3 and AA7050-T7451 Treatment When Loaded with Simple Underloads Spectra

M. Krkoska[1], S.A. Barter[2], R.C. Alderliesten[3], P. White[2], and R. Benedictus[3]

[1]Material Innovation Institute, the Netherlands, m.krkoska@M2i.nl
[2]DSTO, Defence Science and Technology Organisation, Melbourne, Australia
[3]Delft University of Technology, the Netherlands

ABSTRACT *It is well known that variable amplitude loading produces progression marks on fatigue crack surfaces that are related to the loading sequence. These marks are generally a local change in the crack path. In this paper, a number of simple underload loading sequences were used to investigate the influence that underloads have on a crack path and to develop a better understanding of the formation of fatigue striations. The material chosen was 2024-T3 and results were compared to previously investigated 7050-T7451. These two alloys and heat treatments are two very common high strength aluminium alloys and heat treatments used in aircraft design. They represent the underaged and overaged conditions in aluminium alloys. However, AA2024-T3 and AA7050-T7451 aluminium alloys are known to posses different chemical composition, mechanical properties and micro-structures, it was shown that both materials shear essentially similar fracture features corresponding to crack propagation at cycle-by-cycle level. It also appears that despite existing differences, similar failure mechanisms might take place. The exact mechanism of crack path change is still uncertain at the moment; however, it is believed that crack path changes are formed as a consequence of the slip bands formation ahead of crack tip (loading part of the cycle) followed by crack tip collapse (unloading part of the cycle).*

INTRODUCTION

The challenge with fatigue will still be with us in the future, whenever new materials, new design approaches or new production technologies will be applied in design or manufacturing process. Fatigue has been investigated for decades now; but despite the accumulation of knowledge, challenges in prediction of this process still remains, particularly when variable amplitude loading is considered. To improve the predictions, the detailed understanding of mechanisms behind the material's cyclic failure is required, qualitatively and quantitatively. Fractography has already proven its indispensible role in this process and it is still believed to be one of the fundamental tools for fatigue failure investigations. [1]

The interest of visual examination regarding fatigued components could be dated back to 1840s, when Glynn [2] sketched the fracture surface highlighting a "fibrous" structure, as he interpret it. It took another 90 years until the first photograph with the description of a fracture surface was published by Gough [3] in 1930s, reflecting contemporary knowledge on the subject. Another 30 years passed until Forsyth [4] proposed the idea of one-to-one correlation between loading cycle and striation. This

was later convincingly confirmed by Ryder in 1958 [5] for intermediate crack lengths (and stress intensity levels). Subsequently, extensive work has been done in attempt to create general models for fatigue crack advancement. Nowadays, two basic models of crack propagation are generally accepted as a result of those attempts; although, it is also recognized that fatigue is a fairly complex phenomenon and several mechanisms have to be taken in consideration (loading parameters, residual stress at the crack tip, closure mechanisms, strain hardening, crack tip irregularities, environment etc.). Laird proposed the model in 1967, which could be understood as crack tip blunting (loading) and crack tip resharpening (unloading) [6]. Other researchers reviewed this model (supported by extensive fractographic evidence) and they proposed the modification to this model with essentially a very similar concept of slip bands movement at the crack tip [7, 8 and 9]. Neumann [10, 11] approached the problem by incorporating slip processes differently and he proposed a model in which crystallographic cleavage is also involved. Other models for crack propagation could be roughly considered as a modification of these two.

Recently, an interesting model was proposed by White et al. derived from fractographic work. White et al studied the influence of simple underload cycles on crack propagation in AA7050-T7451 aluminium alloy [12, 13]. It was well known that crack propagation and fracture surface appearance produced by variable amplitude loading are different to those produced by constant amplitude loading. The variable amplitude loading usually creates complex fracture surface that contain various distinct features including ridges, depressions and fissures (at shorter to intermediate stress intensity levels). These features were observed before by several other researchers and they are fairly well documented in literature; however, White et al. showed the link between applied load and local crack path changes leading to creation of ridges on one side of the fracture surface and creation of depressions (and possibly fissure) on the matching side. Moreover, depressions and fissures shown to be always pointed in direction of main crack tip and associated with specific surface micro-plane. These observations lead to proposition of the model in which the slip band decohesion at the crack tip and subsequently the crack tip collapse are considered to be the fundamental mechanisms.

The same pattern of loading can produce a pattern of progression marks that have differences from material-to-material or from heat treatment-to-heat. The materials AA2024-T3 and AA7050-T7451 represent high strength aluminium alloys and heat treatments (underaged and overaged conditions) that are commonly used in structures. It was a great deal of interest to re-exanimate the AA2024-T3 alloy. Fractographic observation from crack path changes triggered by reversed underloads for AA2024-T3 are discussed in the paper and compared to those observed on AA7050-T7451 aluminium alloys tested under similar conditions.

EXPERIMENTAL

Testing procedure

A set of load sequences that contained fully reversed underloads in combination with constant amplitude cycles was designed in order to investigate the effect of its size, spacing and grouping. Figure 1 provides a schematic illustration of all sequences used in test program. All tests were performed employing a 100 kN MTS servo hydraulic machine at a frequency of 10Hz in ambient environment (air, temperature).

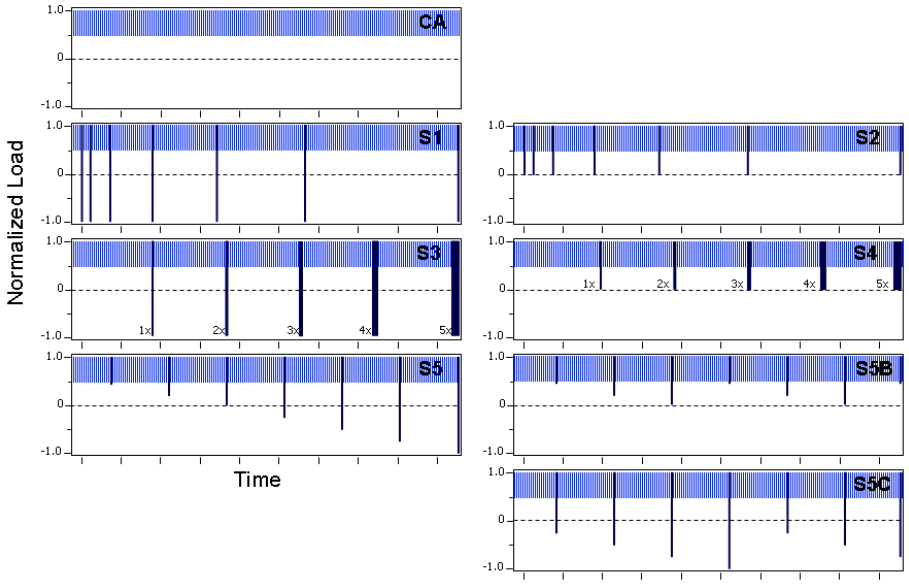

Figure 1. Schematic illustration of all load sequences used in testing program

The load sequence labelled as CA consisted of constant amplitude (CA) cycles with a maximum load that produced a nominal net section stress of 200MPa and a stress ratio ($R=R_{min}/R_{max}$) equal to 0.5.

The load sequences labelled as S1 and S2 consisted of single fully reversed underloads separated by varying number of CA cycles (10, 20, 30, 50, 80 and 130). Fully reversed compressive loads with stress ratio R=-1.0 were applied in sequence S1 while reversed underloads with a stress ratio R=0 were applied in sequence S2 (low R cycles). Sequence S3 and S4 consisted of grouped underloads, increasing subsequently in amount from 1 to 5, separated by 100 CA cycles. A similar logic was adopted for these sequences as for S1 and S2: S3 contains fully reversed compressive loads with stress ratio R=-1.0, while S4 contains reversed underloads with a stress ratio R=0. The load sequence S5 consisted of single fully reversed underloads progressively increasing in magnitude (stress ratio R: 0.45, 0.25, 0, -0.25, -0.5, -0.75 and -1.0) separated by 100 CA cycles. This testing sequence was modified by selecting either only positive underloads, as in sequence 5B (stress ratio R=0.45, 0.25 and 0) or by selecting only negative underloads as in sequence 5C (stress ratio R=-0.25, -0.5, -0.75 and -1.0) separated by CA cycles like in sequence 5.

Test specimen

Flat, dogbone shaped specimens were machined from AA2024-T3 sheets with a length of 177mm, a thickness of 3.2 mm and a width of 40mm. The reduction in width was introduced by a radius of 100mm machined on both sides (to give net width of 25mm). Additionally, the U-shaped notch of 0.1mm wide and 0.25mm deep with semicircular tip was machined at one of the sample's side (using electro discharge machining), tom propagate a crack in LT direction. This specimen geometry gives an initial stress concentration (K_t) equal to 5.54. Figure 2 provides all details on specimen's geometry as used in test programme.

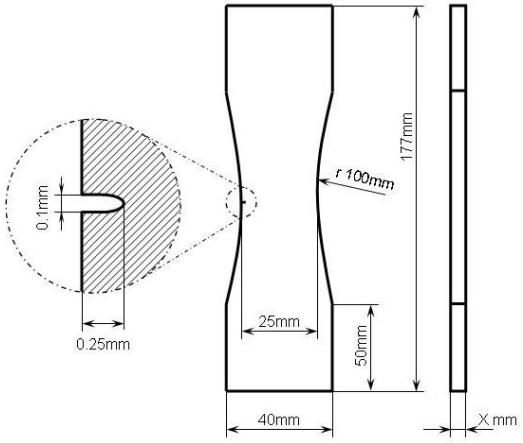

Figure 2. Schematic illustration providing specimen geometry and dimensions

Fractography

A JOEL JSM7500F scanning electron microscope with secondary electron detector was employed in the fractographic investigation.

FRACTOGRAPHIC OBSERVATIONS AND DISCUSSION

Fracture surface features obtained from AA2024-T3 aluminium alloys will be discussed in the following section. Figure 3 shows the difference in fracture surface appearance (on macro-level) of AA2024-T3 and AA7050-T7451 aluminium alloys tested under similar testing conditions due to differences in microstructures.

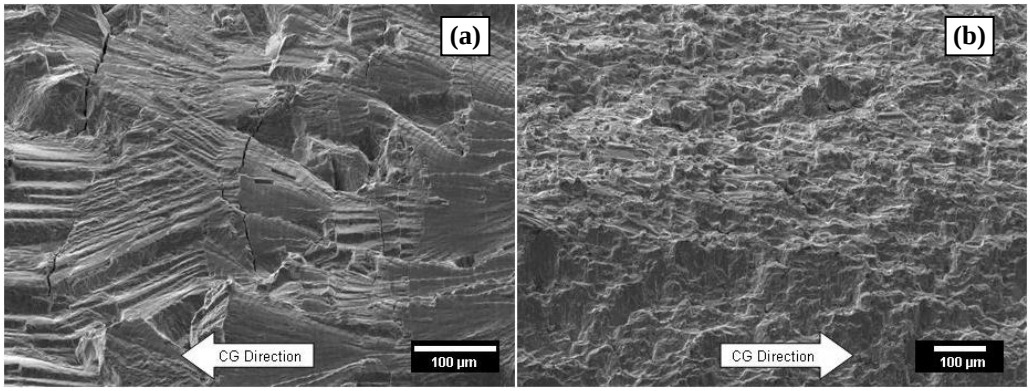

Figure 3. Fracture surface appearance of (a) AA7050-T7451 and (b) AA2024-T3

Although, these alloys posses differences in chemical composition, mechanical properties, micro-structures, etc., it will be shown in this paper that both materials shear very similar features during crack propagation and particularly the crack path change on cycle-by-cycle level seems to operates on very similar mechanism.

General fracture surfaces of all investigated specimens tested under all testing sequences appeared to be oriented normal to the loading direction (or very close to this direction) from very edge of the notch. Crack arrest marks could be easily recognized from very beginning (notch edge) of the crack propagation, revealing the position of the crack front corresponding to blocks of underloads. Usually, featureless fracture planes with shallow orientation are reported at this stage. This difference could be explained as a result of fairly high stress concentration level (5.54) due to the starter notch geometry as well as from testing conditions used. An example of fracture

surface appearance as captured at the crack origin of the specimen loaded with the S1 load sequence is shown in Figure 4a. The visibility of crack arrest marks increased at higher stress intensity levels, revealing position of individual underloads as shown in Figure 4b (individual underloads in blocks produced under testing sequence S2).

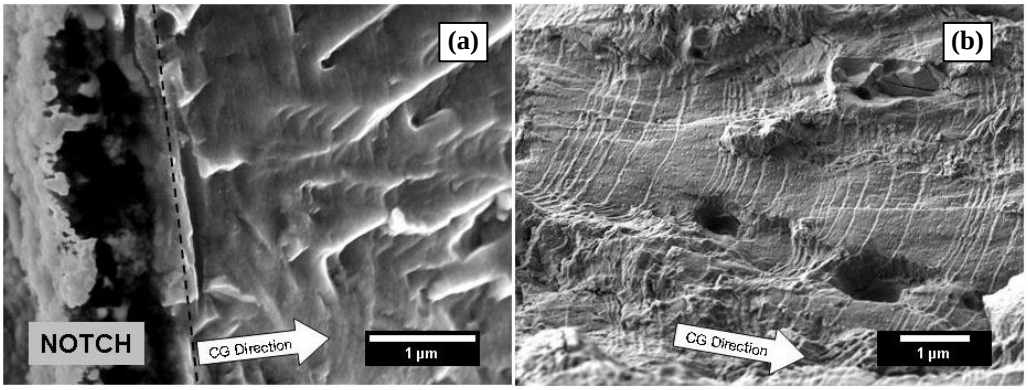

Figure 4. Examples of fracture surface at (a) low and (b) higher stress intensity levels, the load sequences S1 and S2

Figure 5 provides closer look at a typical fracture surface as produced by load sequence S2. The pattern of marks on the fracture surface clearly corresponds to the pattern of underloads used in this sequence (increased number of CA cycles).

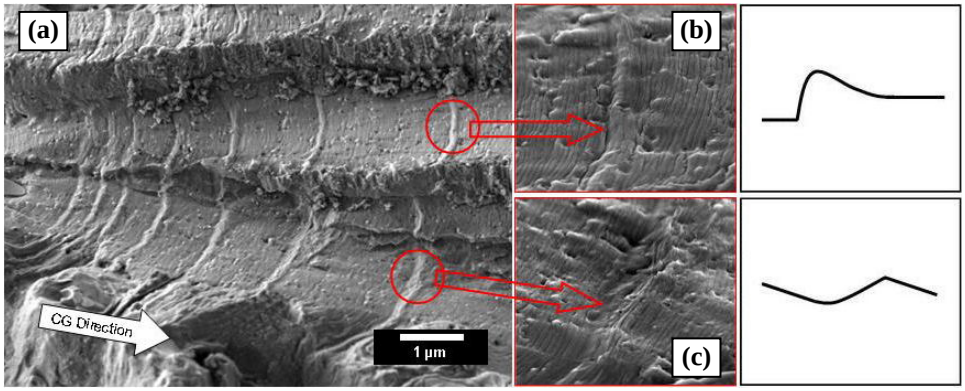

Figure 5. Micrographs highlighting differences in ridge's appearance at differently tilted planes

It was shown by White et al. that each ridge corresponds exactly to the crack tip position at applied underload [12, 13]. They show that the ridge is basically the local the crack path change of crack front resulting in a step-like feature. The exact mechanism of ridge formation is still uncertain; however, it is thought that the ridge is formed as a consequence of the slip band formation ahead of crack tip due to the loading part of the cycle following by crack tip collapse due to the unloading part of the cycle. Subsequent applied CA cycles will force the striations to grow from the top of the ridge [12]. Similar observations were made in current study (Figure 5b and 5c). Interestingly, the geometry of the ridge and direction of CA striations seems to vary depending on its local position, particularly degree of tilting for local fracture plane seems to be important parameter (detail in Figure 5b and 5c). The ridge formed on plane orientated normal (more or less) to the loading direction revealed ductile, round-like appearance with striations growing from its top down-wards forming trailing face of the "bump" and then levelling up approximately to the original plane (before ridge). On the other hand, the ridge formed on plane tilted away from normal direction to the loading direction revealed tearing-like ridge, with striations growing

from its top (disturbed at first) in direction parallel to original plane (before ridge). In this case, no “bumpy” ridge was formed rather step-like crack path change was created.

The examples of fracture surfaces with its characteristic appearance as captured for specimen loaded with load sequence S3 and S4 are shown in Figure 6a.

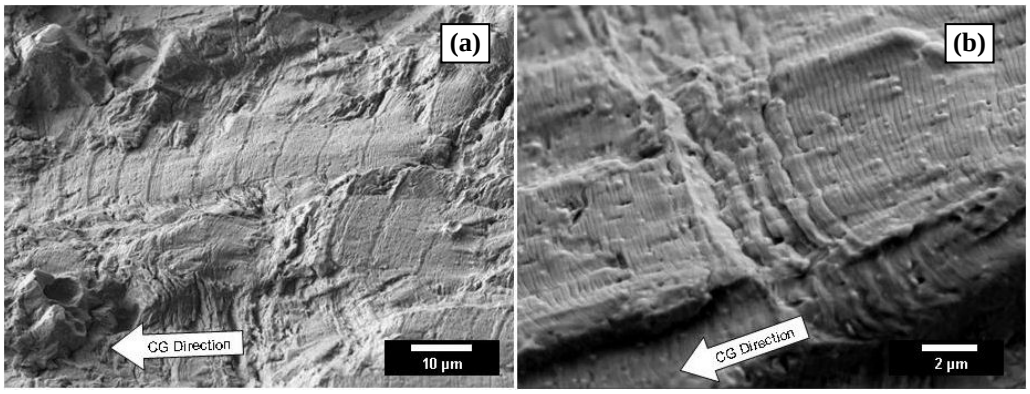

Figure 6. Examples of fracture surface appearance produced with grouped underloads, the load sequences S3 and S4

The pattern of marks on fracture surface also clearly corresponds to pattern of underloads as used in testing sequence, revealing features that appear to be groups of larger striations. Figure 6b provides a closer view on the fracture surface, strictly speaking on the five-larger-striations-to be features at the position of five successive underloads. It is immediately visible that the last “striation” differs from previous four in shape and size; and it seems to be more a crack path change rather than a striation, with shape comparable to ridge described above (Figure 6c). As a matter of fact, it is believed that all marks were created as ridges by compression and unloading part of the cycle to be exact copies of the last ridge in group (fifth in this case); however, they were crushed down in the process by succeeding underload to form large “striations”. The last ridge was not crushed and therefore retained its shape since tensile CA cycles were applied in succession. [12, 13]

Investigation of magnitude (size) of applied underloads on crack propagation and crack path change was also one of the main interests incorporated in this investigation. Figure 7a show the overview of typical fracture surface appearance as it was observed for specimen loaded with sequence S5. It could be concluded from fractographic observations that observed ridge size corresponded to the magnitude of applied underloads. Ill-formed ridges were formed at the position of positive underloads (R=0.45, 0.25 and 0) while ridges gradually increasing in size were formed at the position of negative underloads (R= -0.25, -0.5, -0.75 and -1.0). This trend seems to be more enhanced with steeply tilted planes. The distance between ridges (crack growth rates) was found to be approximately equal and therefore no acceleration of crack growth due to underload size could be observed. These observations were in good agreement with those reported by White at al. [12, 13] for 7050-T7415 aluminium alloy.

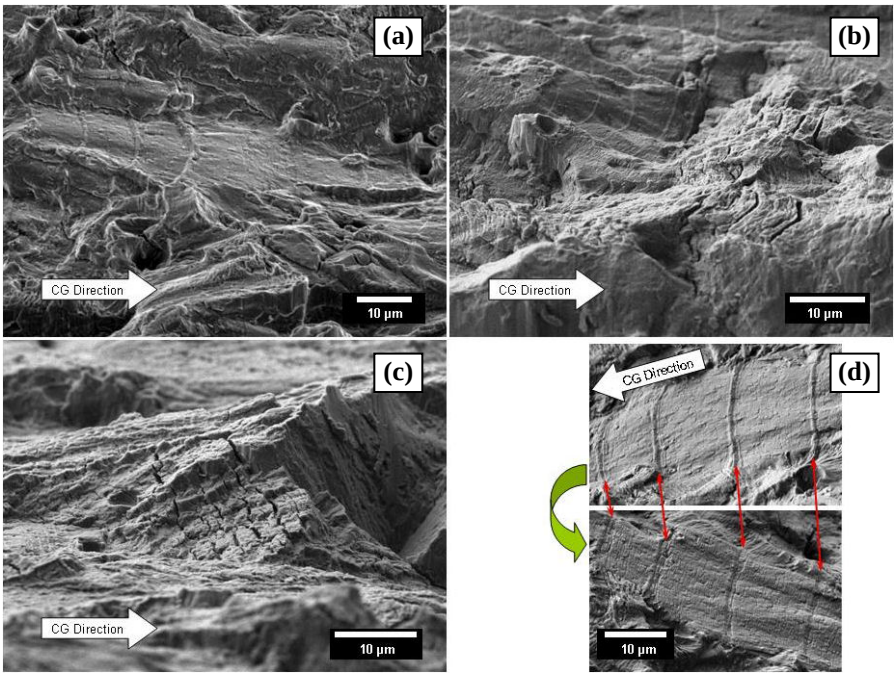

Figure 7. Micrographs of ridges and fissures as obtained for AA2024-T3 Al alloy, (a) altering size of the ridges corresponding to the magnitude of loading, (b) the ridges and fissures that occur at specific local planes, (c) randomly developed fissures with respect to the loading, (d) matching surfaces with perfectly matching ridges and fissures.

Depressions and fissures were also observed to form on the fracture surfaces, always pointed in direction of main crack tip and so occur on specifically tilted planes only. A typical example is shown in Figure 7b, in which the ridges and fissures are captured as they were observed on planes tilted away (ridge) and towards (depressions, fissures) the crack tip origin. Since the ridges and fissures are formed on opposite planes, they can be easily matched together as shown in Figure 7d. Cracks propagating out of the main crack plane (fissures) were found to occur more or less randomly, in regards to the loading pattern as seen in Figure 7b and 7c. This finding is in disagreement with observations made by White at al. [12] (loading dependent results) and McEvily [14] (evenly distributed fissures). White et al reported that fissures tend to occur more likely at the position of underloads separated with the larger CA block and also at the position of last underloads in the case of their grouping. Clearly the behaviour of AA2024T3 and AA7050-T7451 differ when it comes to the out of plane cracking (fissuring).

CONCLUSIONS

Fracture surface and crack paths are known to be affected by applied loading and therefore they appears differently when loaded under variable and constant amplitude cycles. Generally, complex fracture surfaces are observed composed of striations and crack path changes (like ridges, depressions, fissures). Despite the fact that AA2024-T3 and AA7050-T7451 aluminium alloys are known to posses different chemical composition, mechanical properties and micro-structures, it was shown that both materials shear essentially similar fracture features corresponding to crack propagation at cycle-by-cycle level. It also appears that despite existing differences, similar failure mechanisms might take place. Observations regarding crack path

changes as observed for AA2024-T3 and AA7050-T7451 could be summarized as followed:

- the path changes were systematic and related to the load sequences in both alloys resulting in formation of ridges and depressions/fissures
- degree of tilting for local fracture plane seems to be important parameter that determine the ridge geometry and possible the failure mode (ductile vs. tearing-like ridge)
- a ridge could be compressed if another underload is applied in succession forming striation-like mark
- the ridge size seems to be sensitive to applied underload; larger underload will form larger ridge (particularly true for negative loads and inclined planes)
- no acceleration effect was observed for applied underloads level and tested sequences
- depressions and fissures were also observed on specifically tilted planes only and always pointed in direction of main crack tip
- fissures were found to occur more or less randomly, in regards to the loading pattern

The exact mechanism of crack path change is still unknown at the moment; however, it is believed that a ridge is formed as a consequence of the slip band formation ahead of crack tip due to the loading part of the cycle following by crack tip collapse due to the unloading part of the cycle. This issue is still a matter of investigation

ACKNOWLEDGEMENT

This research was carried out under the project number MC2.06269 in the framework of the Research Program of the Materials innovation institute M2i

REFERENCES

1. Schijve J. (1999) *Fat. and Fracture of Eng. Mat. and Str.* **22**, 87.
2. Glynn J. (1844) *Minutes Proc. Inst. Civ. Eng., London* **3**, 202-03.
3. Gough H.J. (1926) *The Fatigue of Metals,* Ernest Benn Ltd., London.
4. Forsyth P.J.E. (1957) *Technical Note MET* **257**, Royal Aircraft Establishment, Farnborough, U.K..
5. Ryder D.A. (1958) *Technical Note MET* **288**, Royal Aircraft Establishment, Farnborough, U.K.
6. Laird C. (1967) *ASTM STP 415*, p.131
7. Tomkins B. and Biggs W.D. (1969) *J. of Mat. Science* **4**, 532-538.
8. Krasowsky A.J and Stepanenko V.A. (1979) *Int. J. of Fracture,* **15**, pp.203-215.
9. Wanhill R.J.H. (1975) *Met. Trans. A*, **6A**, 1587-1596.
10. Neumann P. (1974) *Acta Metallurgica* **22**, 1155- 1165.
11. Neumann P. (1974) *Acta Metallurgica* **22**, 1167- 1178.
12. White P., Barter S.A. and Molent L. (2008) *Int. J. of Fatigue* 30, 1267-1278.
13. White P. Barter S.A. and Wright C. (2009) *Int. J. of Fatigue,* in press
14. McEvily A. J., Endo M., Cho S., Kasivitamnuay J. and Matsunaga H. (2008) *Materials Science Forum* **567-568,** 397-400